Open Access Library Journal
2024, Volume 11, e11597
ISSN Online: 2333-9721
ISSN Print: 2333-9705

Bridge Impact on Water Behavior: Simulation-Application to the Medjerda River in Tunisia

Youssef Mahjoub[1], Amel Soualmia[1], Azeddine Kourta[2]

[1]Department of Rural Engineering, Water and Forestry, National Institute of Agronomy of Tunisia, Carthage University, Tunis, Tunisia
[2]INSA-CVL, PRISME, University of Orleans, Orleans, France
Email: amel.inat@hotmail.fr

How to cite this paper: Mahjoub, Y., Soualmia, A. and Kourta, A. (2024) Bridge Impact on Water Behavior: Simulation-Application to the Medjerda River in Tunisia. *Open Access Library Journal*, **11**: e11597.
https://doi.org/10.4236/oalib.1111597

Received: April 22, 2024
Accepted: May 28, 2024
Published: May 31, 2024

Abstract

The Medjerda Basin is a crucial hub in Tunisia, grapples with recurring floods, significantly affecting social and economic activities in the region. Flood-induced damages disrupt daily life, jeopardizing homes, agriculture, and businesses. This study delves into the intricate dynamics of hydraulic engineering within the challenging context of the Medjerda River Basin, responding to the global flood crisis. This study investigates channel response under diverse flow scenarios. It employs a novel approach by integrating real-scale and scaled-down numerical models to examine the impact of bridge structures on water behavior, providing valuable insights for watercourse management strategies. Simulations reveal distinct behaviors in varying velocities and surface water heights. For real-size models, an inlet velocity of 1 m/s and a water depth of 3 m are considered. In small-size models, conditions involve an inlet velocity of 0.1 m/s and a water depth of 13 cm. The use of both real-scale and scaled-down models, guided by the Froude similarity principle, offers a comprehensive analysis of water dynamics around bridge structures. The investigation seeks to uncover apprehension into the wall shear changes, velocity fields, and hydraulic properties under these conditions. The primary focus is on understanding the water behavior in the channel under varying velocities and surface water heights and assessing the impact of existing bridge structures on water properties. The study will compare numerical calculations to real-world observations in a geometrically reduced model, refining the numerical resolution through practical experimentations. Results from the simulations provide an understanding of water behavior in the Medjerda River, offering valuable insights into the variability of velocity fields. This research contributes to essential knowledge for developing a mul-

tidisciplinary approach that bridges hydraulic engineering, environmental conservation, and urban planning, in the face of changing conditions.

Subject Areas

Hydrology

Keywords

Velocity, Water Behavior, Medjerda, Numerical Modeling, Flood Response

1. Introduction

The realm of free-surface hydraulics holds significant implications for hydraulic management, seamlessly integrating with our hydrodynamic modeling approach [1] [2] [3]. In this broader context, this study focuses on the specific infrastructure in Boussalem, emphasizing the paramount need to understand the intricacies of free-surface hydraulics in this particular location [1]. Moving from this general overview, we delve into the interplay of variables such as channel geometry, flow velocity, and bridge configuration within the studied infrastructure. Our hydrodynamic models are designed to provide a comprehensive insight into the potential impact of the structure on water dynamics, shedding light on specific issues that warrant attention.

This intersection of hydraulic principles with advanced hydrodynamic modeling not only underscores the interdisciplinary nature of our study but also emphasizes the need for a nuanced understanding of the underlying physics [2] [4] [5].

Navigating the complex interdependence between hydraulic systems and surface water dynamics, our scientific endeavor aims to bridge the gap between theoretical knowledge and practical implications in the realm of infrastructure development [2] [4] [5]. By narrowing our focus to the specific challenges within Boussalem's infrastructure, we aim to contribute meaningfully to this critical intersection.

The primacy of hydraulics is fully manifested in our assessment, highlighting the crucial importance of the structure within the city of Boussalem [3]. Positioned along Route RN6 and connecting the north to the south of the city, this structure holds dual significance. Firstly, its location within the city imparts strategic importance to local hydraulic management. Simultaneously, by playing a pivotal role in linking the upper Medjerda Valley to the rest of the watershed, this structure becomes a key element in regional connectivity [2] [3].

This intersection between local hydraulics and the road network underscores the holistic approach of our assessment, aiming to comprehend the integrated impact of this infrastructure on Boussalem and its hydrological environment. It is within this specific domain that our study identifies a research gap, emphasizing the need for tailored insights into the challenges posed by the intricate inte-

raction of hydraulics and infrastructure.

Building upon our study's foundation, our methodology advances by creating real-scale numerical models of the Boussalem infrastructure. These models simulate and dissect its impact on water behavior. To bolster our analysis, we compare these real-scale models with reduced-scale counterparts, guided by the Froude similarity principle. This comparative framework systematically examines hydraulic patterns at different scales.

This innovative methodology not only comprehensively understands the structure's influence on water dynamics but also addresses the identified research gap. Using the Froude similarity principle, we aim to extend this research to our INAT laboratory canal, exploiting its unique features. This extension seeks to refine our techniques, contributing to a nuanced understanding of the interplay between infrastructure and hydraulics, thus filling a critical gap in the existing literature. This approach not only deepens our current study but also sets the stage for ongoing exploration within hydraulic research, contributing to valuable insights into the broader domain.

2. Case Presentation

The Medjerda River Bridge, built in 1983, serves as a modern successor to its historical predecessor, a structure with roots dating back to the French colonial era (Atlas Numérique du Gouvernorat de Jendouba, 2014). Situated at a latitude of +36˚36'04" and a longitude of +06˚37'56", with an altitude of 127 m, the historical bridge includes the Boussalem hydrometric station, identified by the matriculate 1,485,400,180. (See Figure 1)

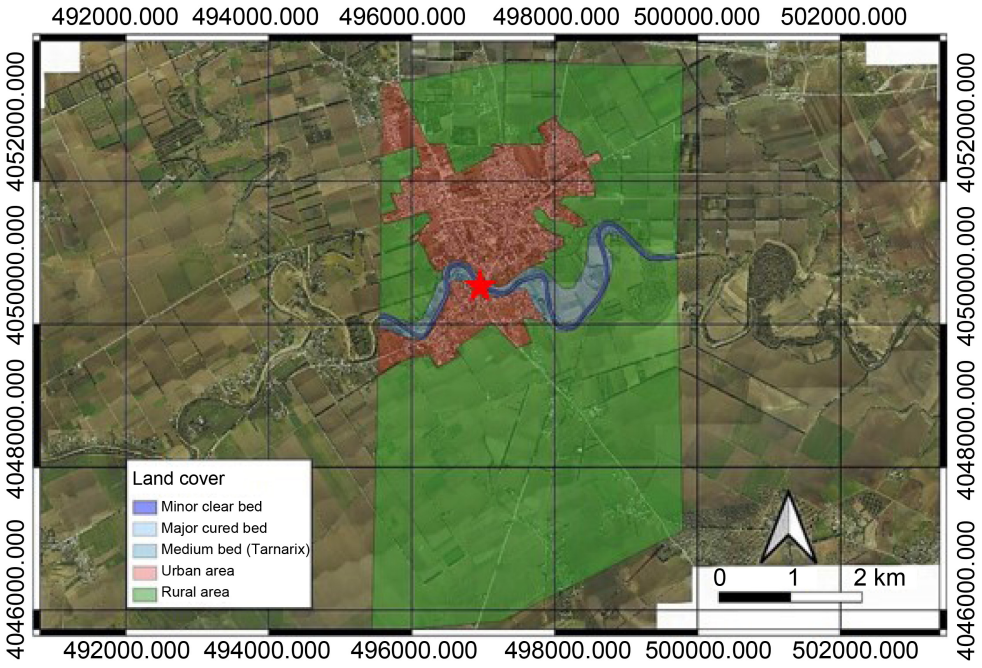

Figure 1. Geographical map of the city of Boussalem situated in the Medjerda River Basin in Tunisia, highlighting the location of the study bridge (red star).

The structure is a variable-height prestressed concrete beam bridge, with the clearance under the structure ranging from 3 to 12 meters. Its total length is 108 meters, divided into 3 equal spans of 36 meters each. The deck consists of prestressed concrete beams, supported by reinforced concrete abutments, and the foundations are constructed using piles (Digital Atlas of the Jendouba Governorate, 2014).

In the past years, recurrent flood events occurred in 2000, 2003, 2004, 2005, 2009, 2012, and 2015. These notable floods resulted in substantial damage in northern part of the country, particularly in the upstream Medjerda basin [3].

The historical flooding incidents experienced by the city, coupled with the bridge's strategic location, establish it as a crucial asset for hydraulic analyses. (See **Figure 2**)

3. Methods

Physical models in Urban Hydraulics offer a comprehensive approach to estimate flow disturbance in diverse infrastructures like pumping stations and sewer systems [6] [7] [8]. Serving a dual purpose, they validate designs before implementation and identify malfunctions in existing facilities [6] [8]. Fixed-bed models, common in urban hydraulics [8], ensure similarity through precise geometric reduction scales. Mobile-bottom models address stabilization, while fixed-bottom models focus on accurate flow reproduction [8]. Constraints on scale prototype realization include geometric precision, material fidelity, time constraints, and associated costs [7] [8] [9].

Figure 2. Field visit snapshot of the bridge (24-12-2023).

3.1. Geometrical, Kinematic and Dynamic Similarities

Ensuring resemblance to the prototype, the physical model must maintain geometric, kinematic, and dynamic similarities, where geometric similarity pertains to scale, kinematic similarity ensures an accurate representation of velocity fields, and dynamic similarity demands constancy in observed ratios [6] [8] [10].

$$E_V = \frac{V_p}{V_M} \tag{1}$$

where

E_V : Velocity scale;

V_p : Real scale velocity;

V_M : Model scale velocity.

Generally

$$E_V = E_l \cdot E_t \tag{2}$$

where

E_V : Velocity scale;

E_l : Length scale;

E_t : Time scale.

The complete similarity of fluid motion between the model and the prototype will only be achieved when the polygon of forces acting on a fluid particle in the prototype is faithfully replicated on the model [6] [8] [10]. For inertia forces, this requirement can be expressed in the form of an equation by applying the expression of the fundamental law of dynamics.

$$\frac{F_p}{F_m} = E_m \cdot E_l \cdot E_t^{-2} \tag{3}$$

where

F_p : Real scale force;

F_m : Model scale force.

3.2. Physical Similitude-Criteria for Designing

In fluid dynamics and hydraulic modeling, achieving accurate scaled-down representations relies on meticulous attention to similarity ratios and dimensionless numbers [8] [10]. These parameters ensure proportional relationships between forces in a model and the full-scale prototype, therefore crucial for faithful fluid reproduction [8] [9] [10]. Despite challenges in selecting specific similarities, the delicate balance between similarity ratios and dimensionless numbers remains pivotal for trustworthy insights into fluid behavior. As designers, our goal is to conduct precise analyses and meaningful tests by maintaining coherence between the real-scale bridge and the 1/100 geometric small-scale prototype, and so allowing numerical validation and comparison with laboratory results.

3.3. Hydrodynamic Model

In the field of fluid dynamics, numerical modelling stands out as a powerful

computational tool for analyzing systems characterized by fluid flow, heat transfer, and associated phenomena such as chemical reactions [8]. This study synthesizes our exploration for fundamental aspects of numerical modelling, focusing on Reynolds decomposition, mass conservation Equation (4), and momentum balance Equation (5):

$$\frac{\partial \rho}{\partial t} + div\left(\rho \cdot U\right) = 0 \tag{4}$$

And

$$\rho \cdot \frac{\partial u_i}{\partial t} + \rho \cdot u_j \cdot \frac{\partial u_i}{\partial x_j} = -\frac{\partial p}{\partial x_i} + \mu \cdot \frac{\partial^2 u_i}{\partial x_i x_j} + \rho \cdot g_i \tag{5}$$

where

ρ : Fluid density;

U: Longitudinal velocity vector;

u_i : The component of the velocity vector in the i direction;

t: Time;

g_i : The component of the gravity vector in the i direction;

μ : Viscosity;

p: Static pressure;

x_i : x component in the i direction.

We begin with an in-depth analysis of Reynolds decomposition, employing essential statistical tools for the treatment of experimental data and theoretical calculations. This approach allows us to decompose each characteristic of the flow into an average value and a fluctuating value. Next, we formulate the mass conservation equation for a permanent flowing regime and an incompressible fluid. This equation provides a precise mathematical formulation of the mass law conservation for a material control volume.

The conservation of momentum is addressed using the momentum balance equation, based on Newton's second law. This equation establishes the connections between fluid attributes and its motion relative to underlying causes [8] [10] [11].

Finally, we delve into Reynolds-Averaged Navier-Stokes (RANS) equations, emphasizing the effect of turbulence on mean flow properties. We present a derivation that includes an advection term created by the fluctuating movement of turbulent momentum, interpreted as the Reynolds tensor:

$$\rho \frac{\partial \overline{u_i}}{\partial t} + \rho \overline{u_j} \frac{\partial \overline{u_i}}{\partial x_j} = -\frac{\partial \overline{p}}{\partial x_i} + \frac{\partial}{\partial x_j}\left(\overline{\tau_{ij}} + \overline{\tau'_{ij}}\right) + \rho g_i \tag{6}$$

where

τ_{ij} : Tensor viscous stresses;

$\overline{\tau'_{ij}}$: Reynolds stress tensor.

This synthesis underscores the need for physical models in urban hydraulics, emphasizing their validation and refinement. Fixed-bed models dominate, considering constraints such as geometry, material, time, and financial considera-

tions. The importance of achieving physical similitude is highlighted, concluding with a focus on the crucial role of numerical modelling and Reynolds-Averaged Navier-Stokes equations in these contexts.

4. Numerical Modelling

4.1. Geometrical Setup

The geometries of the small-sized and large-sized models were used for numerical simulations (see Figure 3). Their dimensions were setup as in Table 1. They are geometrically similar and the scale ratio of length is equal to 100.

4.2. Model Mesh Setup

Numerical modelling has been selected as the physics preference in the mesh creator, with a preference for the fluent solver and a linear element order. The growth rate is set at 1.2, with element size of 2 cm for the small-scaled model and a curvature normal angle of 18˚. (See Figure 4)

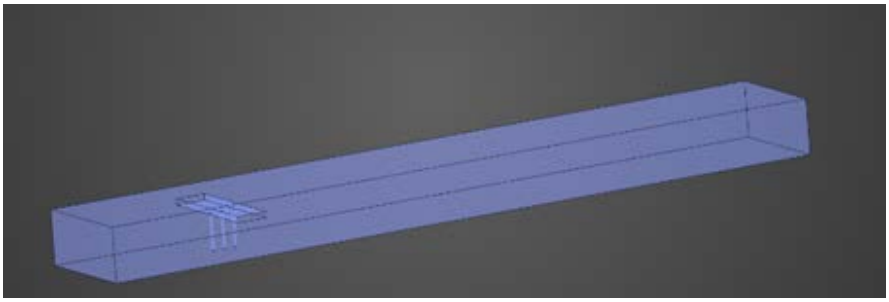

Figure 3. Imported geometry (image captured from ANSYS visual interface).

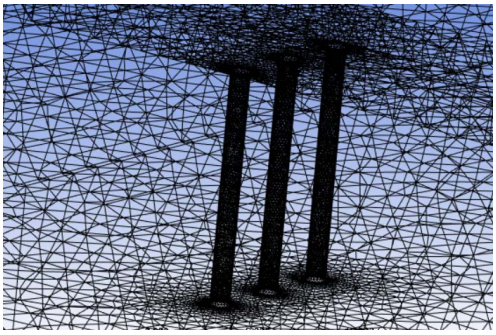

Figure 4. Mesh graphical results (snap taken from ANSYS Meshing interface).

Table 1. Geometric setups for the small-sized and the large-sized simulations.

	Real-Sized Model	Small-Sized Model
Channel Length	250 m	250 cm
Channel Width	80 m	80 cm
Depth of Water	3 m	3 cm
Diameter of Pylons	1 m	1 cm

Additionally, the meshing process was further refined using peers neighbors to unveil finer details around the structure. This meticulous refinement ensured that the transition between elements was smooth, enhancing the clarity of the results near the structure. The chosen options resulted in a mesh containing 65,748 nodes and 346,389 elements.

4.3. Boundary Condition Setup

At the inlet boundaries, pressure-inlet conditions were specified with uniform water velocity and level distributions. The velocity scale ratio of ten, equivalent to the square root of the length scale ratio (100), ensured compliance with Froude number similarity. Downstream outlets featured pressure-outlet conditions with water surface levels set divided by 100 for the small size. Normal gradients of dependent variables were set to zero, extrapolating values from the interior domain. To establish the atmospheric pressure boundary condition, an open pressure condition was employed for simulation. Wall boundary conditions were applied to the remaining surfaces.

In this section, geometric setups for small and large models were presented, maintaining a scale ratio of 100. The ANSYS fluent mesh configuration included 65,748 nodes and 346,389 elements. Boundary conditions were carefully set to ensure Froude number similarity. These parameters establish a realistic foundation for the subsequent numerical simulations.

4.4. Validation/Calibration of the Numerical Model

The effectiveness of two different turbulence models, k-omega and standard k-epsilon, was assessed for accurately representing turbulence behavior around/behind the pile. Numerical simulations indicated that the k-omega model provided a slightly better fit to the data compared to the k-epsilon model. Previous studies have demonstrated the high performance of the k-omega closure model for boundary-layer flows with strong adverse pressure gradients or flow separations [11] [12]. Based on this finding, the k-omega turbulence closure was adopted for the entire numerical investigation. Once the turbulence closure (*i.e.*, k-omega turbulence model) was selected, the sensitivity of the results to certain model variables, such as surface roughness of the flume and pile, and fluid viscosity, was examined through a series of numerical experiments.

Once the turbulence closure (*i.e.*, k-ω turbulence model) was selected, the sensitivity of the obtained results to certain model variables was tested by a series of numerical trials. In these trials, the roles of surface roughness of the flume and pile, and the fluid viscosity were tested.

5. Results

In previous sections, we introduced our study's framework and extensively developed our prototype using CFD simulations. This section unveils primary outcomes from geometric and numerical simulations, highlighting the impera-

tive for a more in-depth investigation of the problem.

5.1. Software Output Results

The convergence between the scaled-down model and the full-scale model remains remarkably consistent, particularly at the surface blade level. (See Figure 5) The heights and velocities maintain a relative stability, thereby preserving the ratio in accordance with the Froude similarity. This constancy underscores the robustness of our approach, demonstrating the results coherence between the scaled-down prototype and the full-scale system.

The persistent agreement between the scaled-down and full-scale models, specifically at the water surface level, is succinctly captured in Table 2, encapsulating the stability of heights and velocities in adherence to the Froude similarity ratio.

In Figure 6, a crucial detail emerges. In fact maximum shear stress concentrates near the piers, particularly on their sides, in both the small-scale (b) and the real-scale models (a). This deviates from a uniform distribution, indicating a more focused erosive force. The culprit behind this phenomenon is the flow separation that occurs around the piers. As the water encounters the pier, it's forced to deviate, creating zones of high velocity along the sides and a region of recirculation with slower moving water behind the pier. This interaction between the main flow and the recirculation zone generates the concentrated shear stress responsible for the observed pattern. Interestingly, the downstream area of the second pier experiences the strongest impact, with values around 21 Pa compared to 13 Pa near the first pier and minimal influence at the third, for both simulations. This pattern translates to a heightened risk of erosion, especially on pier sides, and potentially influences sediment transport patterns downstream, particularly near the second pier.

Figure 7 reveal the evolution of x-direction velocity u near the water surface. The overall trend remains consistent with some nuances. Values reach their

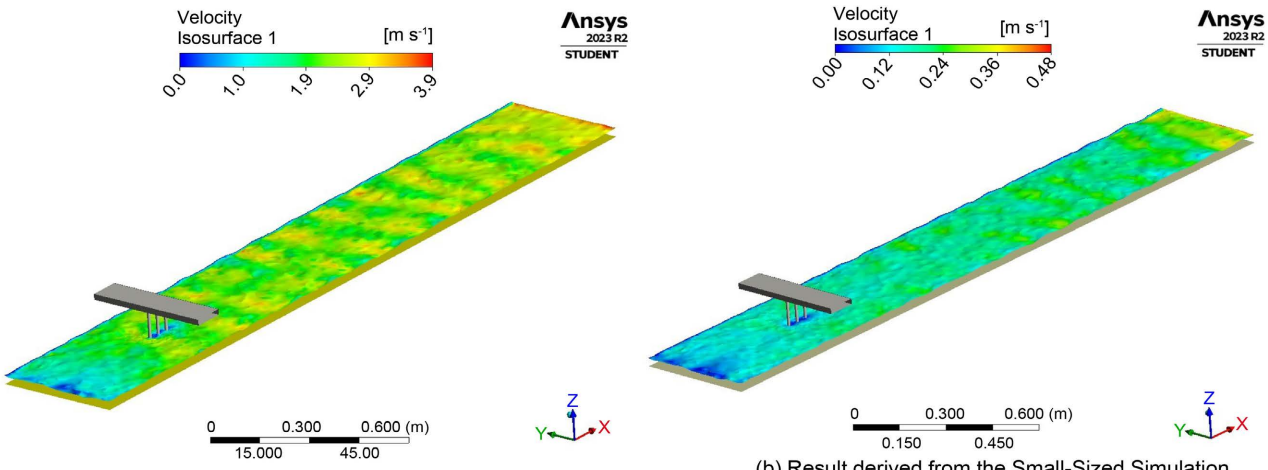

(a) Result of the Large-Sized Simulation.

(b) Result derived from the Small-Sized Simulation according to the Froude Law.

Figure 5. Consistency of scaled-down and full-scale models: surface blade parameters in Froude similarity.

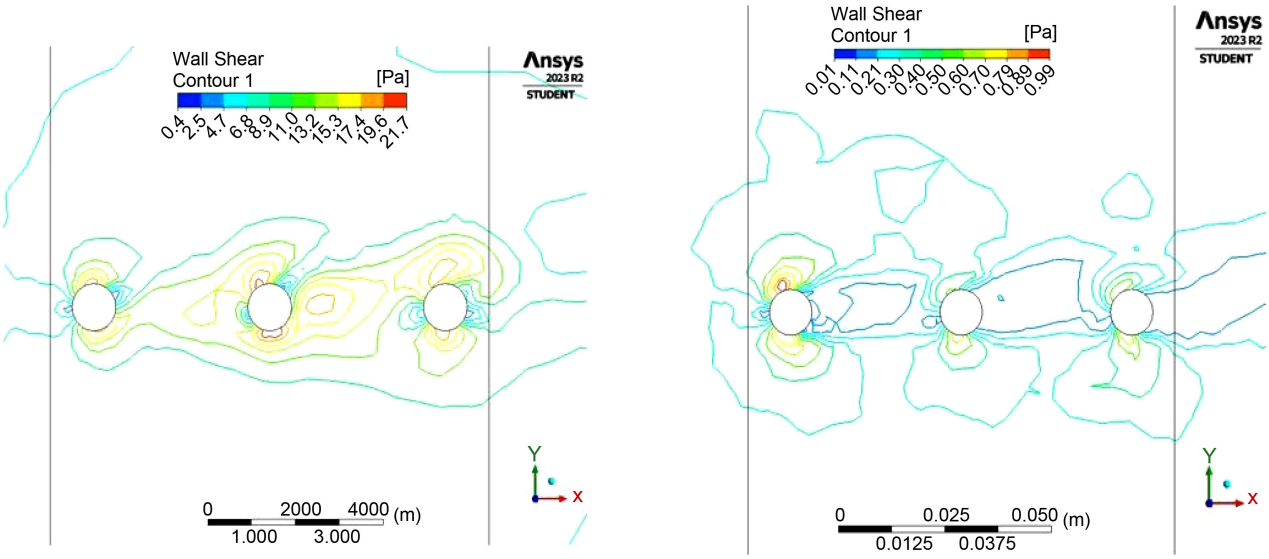

(a) Result of the Large-Sized Simulation.

(b) Result derived from the Small-Sized Simulation according to the Froude Law.

Figure 6. Shear stress (Pa) at the bottom for the large sized (a) and the small sized (b) models.

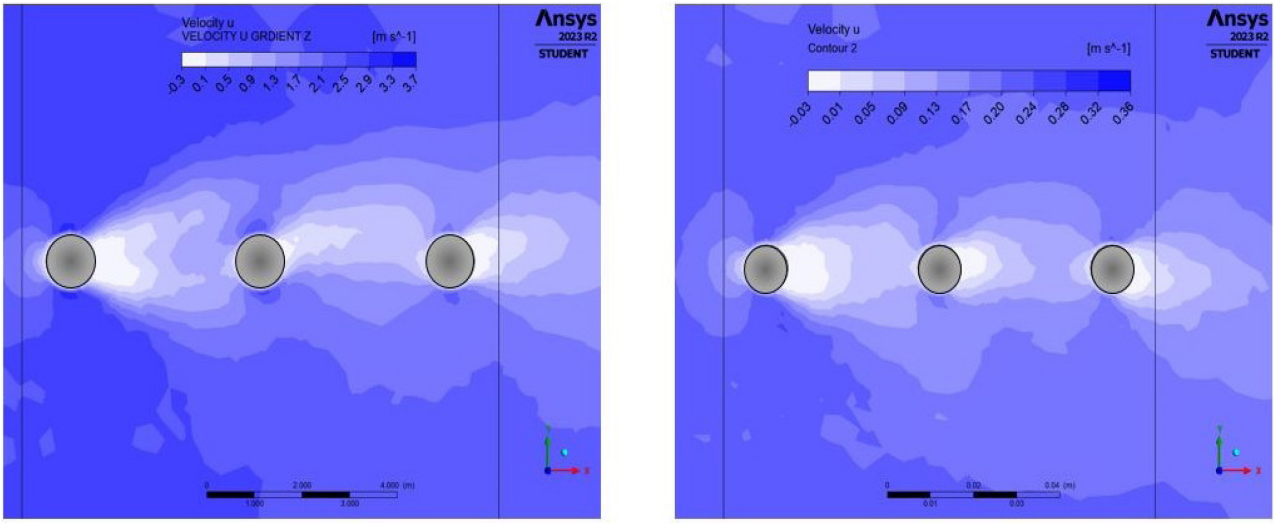

(a) Result of the Large-Sized Simulation.

(b) Result derived from the Small-Sized Simulation according to the Froude Law.

Figure 7. Contour of X-direction velocities differences between the large sized (a) and the small sized (b) simulations according to the Froude law.

Table 2. Summary of output parameters related to the water surface.

	Real-Sized Model	Small-Sized Model
Average Velocity	2.8 m/s	0.28 m/s
Mean Height	3.02 m	0.03 cm
Minimum Water Level Height	2.2 m	0.023 m
Maximum Water Level Height	3.83 m	0.038 m

minima on the sides and increase downstream of each pier for both models (a) and (b). The value downstream of the first pier is lower and increases downstream of each subsequent pier.

A downward flow emerges due to the negative stagnation pressure gradient near the upstream side of the pier. This pressure gradient arises as the flow accelerates around the pier, causing a region of low pressure on the upstream side. Interactions with the horizontal boundary layer separation, where the flow separates from the riverbed, give rise to a vortex system. This vortex system, characterized by swirling currents, is responsible for the scouring (erosion) at the base of the pier. Recirculation zones appear after each pier and reach velocities of 0.3 m/s in the real model (0.03 m/s in the reduced model). These recirculation zones form because the flow separates behind the pier, creating a region of slow-moving or stagnant water. These zones occupy a larger surface area near the first obstacle and decrease in size downstream as the flow has already been disturbed by the upstream pier.

The analysis of shear stress, sediment transport, and velocity gradients reveals heightened erosion potential near pillars, impacting scour patterns. Practical applications can draw from these insights, guiding effective strategies for mitigating sediment-related concerns in bridge pier scenarios.

Following the insights gleaned from shear stress distribution (Figure 6) and velocity contours in Figure 7, Figure 8 dives deeper by showcasing the velocity vectors near the water surface for both the small-scale (b) and the real-scale models (a). These vectors represent the direction and the relative magnitude of water movement in the horizontal plane (x-direction). Analyzing their patterns, particularly around the piers, reveals similar flow directions behind the first piers for both models. However, a key difference emerges behind the last pier. While the small-scale model (b) exhibits more uniform vectors indicating a

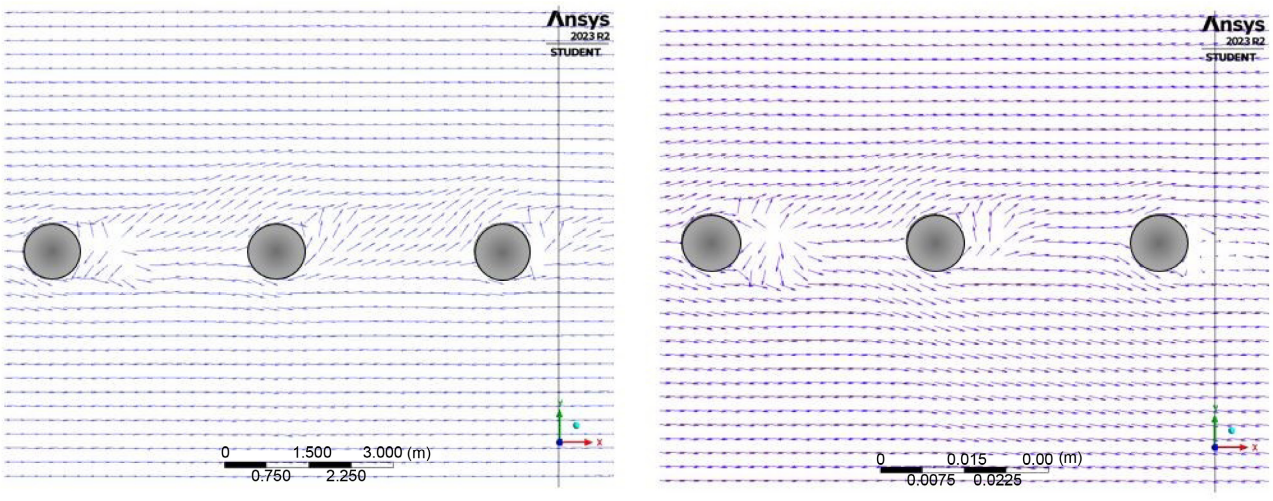

(a) Result of the Large-Sized Simulation.

(b) Result derived from the Small-Sized Simulation according to the Froude Law.

Figure 8. Velocity vector near water surface.

relatively straight flow path, the real-scale model (a) shows more divergent vectors suggesting a more turbulent flow. This variation could be attributed to the scale effects associated with the Froude law. By combining the analysis of velocity vectors and the shear stress distribution, we gain a more holistic understanding of the flow dynamics and the potential scour patterns around the piers.

5.2. Discussion

Figure 6 depict shear stress contours for small and large simulations. Near the pier, the figures show the highest predicted bed shear stress values. If surpassing the critical shear stress for particles, sediment transport and local scour may occur in this region.

Figure 7 shows contours of the x-direction velocity difference between the large simulation model and the small-scale physical model, adhering to Froude law. The flow slows near the cylinder, leading to water accumulation upstream. Around structures, the flow accelerates, halting at the pier face. Stagnation pressures peak near the surface due to maximum deceleration, diminishing downward. In response to the downward pressure gradient at the pier face, flow reaches a maximum just below the bed level. Notably, the overall velocity ratio is maintained near the piers. In conclusion, Figure 8 illustrates the x-direction velocity vectors for both the small and the large models, revealing similar patterns with distinct values in the vicinity of the piers. The presence of recirculation zones after each pier is also observed, which are more significant at the first obstacle and diminish downstream.

This constancy underscores the robustness of our approach, demonstrating the coherence of results between the scaled-down prototype and the full-scale system.

Numerical simulations indicate separation zones and vortex systems around both small and large bridge piers, consistent with the study's objectives.

Validation of scale and modeling approaches is observed. In fact, this study contributes to practical scour mitigation strategies, inspiring real-world exploration.

6. Conclusions

In conclusion, this study on hydraulic management, focusing on free-surface hydraulics in the context of the Boussalem infrastructure, has successfully employed an advanced hydrodynamic modeling approach. The integration of hydraulic principles with real-scale numerical models, guided by the Froude similarity principle, has provided valuable insights into the water dynamics surrounding the studied structure.

The CFD simulations confirm the effectiveness of our scaled-down model, maintaining coherence with the full-scale system. Adhering to the Froude similarity ratio at the surface blade level ensures relative reliability in capturing water behavior complexities. The Analysis of water surface parameters analysis shows

agreement between real-sized and small-sized models, revealing heightened erosion potential near bridge piers. Practical applications include strategies for sediment concerns in bridge pier scenarios. The validated methodology and adherence to the Froude principle lay the groundwork for ongoing hydraulic research, emphasizing informed decision-making in infrastructure development in Boussalem and similar contexts.

Acknowledgements

The authors extend profound gratitude to the dedicated teammates at the INAT and PRISME laboratory, whose collaborative efforts have enriched my academic journey and contributed significantly to the success of our shared endeavors.

Conflicts of Interest

The authors declare no conflicts of interest.

References

[1] Gharbi, M., Soualmia, A., Dartus, D. and Masbernat, L. (2014) A Comparative Analysis of Lajeunesse Model with Other Used Bed Load Models-Effects on River Morphological Changes. *Journal of Water Resources and Ocean Science*, **3**, 61-68. https://doi.org/10.11648/j.wros.20140305.12

[2] Gharbi, M., Soualmia, A., Dartus, D. and Masbernat, L. (2016) Comparison of 1D and 2D Hydraulic Models for Floods Simulation on the Medjerda Riverin Tunisia. *Journal of Materials and Environmental Science*, **7**, 3017-3026.

[3] Hammami, S., Soualmia, A. and Kourta, A. (2023) Analysis and Forecasting Flood Risk Mapping of the Medjerda River at Boussalem Town, in Tunisia. *Engineering & Applied Science Research*, **50**, 3-4.

[4] Hunter, N.M., Bates, P.D., Neelz, S., Pender, G., Villanueva, I., Wright, N.G. and Mason, D.C. (2008) Benchmarking 2D Hydraulic Models for Urban Flooding. *Proceedings of the Institution of Civil Engineers-Water Management*, **161**, 13-30. https://doi.org/10.1680/wama.2008.161.1.13

[5] Talbi, S. H., Soualmia, A., Cassan, L. and Masbernat, L. (2016) Study of Free Surface Flows in Rectangular Channel over Rough Beds. *Journal of Applied Fluid Mechanics*, **9**, 3023-3031. https://doi.org/10.29252/jafm.09.06.25898

[6] Chanson, H. (2004) Hydraulics of Open Channel Flow. Elsevier, Amsterdam.

[7] Tartandyo, R.A., Ginting, B.M. and Zulfan, J. (2023) Scale Effects Investigation in Physical Modeling of Recirculating Shallow Flow Using Large Eddy Simulation Technique. *Journal of Applied Fluid Mechanics*, **17**, 43-59. https://doi.org/10.47176/jafm.17.1.1980

[8] Martaud, M. and Heywood, S. (1999) Les modèles physiques en hydraulique urbaine. *La Houille Blanche*, **85**, 67-74. https://doi.org/10.1051/lhb/1999009

[9] Jasim, R.A., Hussen, W.Q., Abdullah, M.F. and Zulkifli, R. (2023) Numerical Simulation of Characterization of Hydraulic Jump over an Obstacle in an Open Channel Flow. *Journal of Advanced Research in Fluid Mechanics and Thermal Sciences*, **106**, 1-15. https://doi.org/10.37934/arfmts.106.1.115

[10] Aksel, M. (2023) Numerical Analysis of the Flow Structure around Inclined Solid Cylinder and Its Effect on Bed Shear Stress Distribution. *Journal of Applied Fluid*

Mechanics, **16**, 1627-1639. https://doi.org/10.47176/jafm.16.08.1697

[11] Roulund, A., Sumer, B.M., Fredsøe, J. and Michelsen, J. (2005). Numerical and Experimental Investigation of Flow and Scour around a Circular Pile. *Journal of Fluid Mechanics*, **534**, 351-401. https://doi.org/10.1017/S0022112005004507

[12] Larsen, B.E., Fuhrman, D.R. and Sumer, B.M. (2016) Simulation of Wave-plus-Current Scour beneath Submarine Pipelines. *Journal of Waterway, Port, Coastal, and Ocean Engineering*, **142**, Article 04016003. https://doi.org/10.1061/(ASCE)WW.1943-5460.0000338